PHYSICAL REVIEW B **77**, 201303(R) (2008)

Hidden ferromagnetic secondary phases in cobalt-doped ZnO epitaxial thin films

T. C. Kaspar,[1,*] T. Droubay,[1] S. M. Heald,[2] M. H. Engelhard,[1] P. Nachimuthu,[1] and S. A. Chambers[1]

[1]*Pacific Northwest National Laboratory, Richland, Washington 99354, USA*

[2]*Advanced Photon Source, Argonne National Laboratory, Argonne, Illinois 60439, USA*

(Received 25 March 2008; published 7 May 2008)

The origin of ferromagnetism is investigated in epitaxial Co:ZnO thin films which become weakly ferromagnetic after annealing in Zn vapor. Conventional characterization techniques indicate no change after treatment. However, x-ray photoelectron spectroscopy depth profiling clearly indicates the presence of Co(0) in the Zn-treated films; x-ray absorption fine structure is utilized to identify the secondary phase as ferromagnetic CoZn. This work demonstrates that the potential for ferromagnetic secondary phases must be thoroughly discounted, through painstaking materials characterization, before claims of intrinsic ferromagnetism can be made.

DOI: 10.1103/PhysRevB.77.201303 PACS number(s): 75.25.+z, 75.50.Pp, 85.75.−d

Spintronics has the potential to revolutionize electronic devices by effectively utilizing the spin degree of freedom.[1] However, developing the required materials necessary for room temperature operation presents a serious materials physics challenge. Investigation of potential dilute magnetic semiconductor (DMS) materials utilizing semiconducting oxide hosts was motivated by both theoretical[2] and experimental[3] findings of ferromagnetism at room temperature in doped oxides. Despite the enormous body of research that followed,[4–6] no unambiguous demonstration of carrier-mediated ferromagnetism has been made. Disparate and irreproducible experimental results have led to serious doubts as to whether the observed ferromagnetism is intrinsic to the doped oxide system or due to extrinsic effects, such as contamination or phase impurity.[4,7,8] As one example, the reported magnetization values for Co:ZnO range over 2 orders of magnitude (paramagnetic to $<0.05\mu_B$/Co to $>6\mu_B$/Co).[9,10] Recently, we showed that structurally well-defined Co-doped ZnO is not intrinsically ferromagnetic, either in the semi-insulating state or when electronically doped *n* type.[10]

Weak ferromagnetism in Co:ZnO ($0.1-0.3\mu_B$/Co) has been induced by annealing in Zn vapor to diffuse interstitial Zn (Zn_i) into the Co:ZnO lattice.[11–14] The proposed model for ferromagnetism in the presence of Zn_i involves specific defect/donor formation which facilitates electron-mediated Co spin alignment.[11,12] Subsequent annealing in oxygen removes Zn_i, returning the material to the insulating, nonferromagnetic state.[11,12] These results thus suggest that defects specifically associated with Zn_i are necessary to realize ferromagnetic ordering, and introduction of *n*-type carriers by other means is not sufficient.

In this paper, we further explore the origin of ferromagnetism in epitaxial Zn_i:Co:ZnO thin films which have undergone a similar Zn vapor treatment. Initial materials characterization indicated no phase segregation or Co reduction occurred, implying the ferromagnetism ($\sim 0.05\mu_B$/Co) is intrinsic to Zn_i:Co:ZnO. However, a more careful analysis correlates the observed ferromagnetism to the presence of Co(0) in the form of trace amounts of ferromagnetic CoZn ($\sim 1.5\mu_B$/Co). These results emphasize the vigilance required in materials characterization before intrinsic ferromagnetism can be definitively attributed to the substitutionally doped oxide phase.

Epitaxial $Co_xZn_{1-x}O$ thin films were deposited by pulsed laser deposition on single crystal *c*-plane $Al_2O_3(0001)$ and *r*-plane $Al_2O_3(01\bar{1}2)$ substrates, at 475 °C in 1×10^{-3} Torr O_2, from a sintered $(CoO)_{0.1}(ZnO)_{0.9}$ target, as described previously.[10] Treatment in Zn vapor was accomplished by sealing the films in an evacuated quartz tube containing Zn metal. The sealed ampoule was then heated in a tube furnace from room temperature to 600 °C, held at temperature for 5 h, and then cooled to room temperature. In contrast to previous work,[11,12] the diffusion process was found to be irreversible; reoxidation for 2 h at 500 °C in flowing O_2 did not alter the magnetization or resistivity of the Zn-treated film.

Figure 1(a) presents the magnetic hysteresis loops, taken by vibrating sample magnetometry (VSM) at room temperature, for an *a*-$Co_{0.1}Zn_{0.9}O$ film deposited on *r*-Al_2O_3. The as-deposited film is insulating ($>10^5$ Ω cm) and shows negligible ferromagnetism, as expected.[10] However, after annealing in Zn vapor at 600 °C for 5 h, a distinct increase in magnetization occurs, resulting in a saturation moment of $0.05\mu_B$/Co (2.4×10^{-5} emu total moment). This ferromagnetic signal is substantially larger than the negligible moments previously observed for *n*-Co:ZnO,[10] and is consistent with ferromagnetism observed in other Co:ZnO treated in Zn vapor.[12,13] Concurrently, the film resistivity after Zn treatment is substantially reduced to 0.03 Ω cm, presumably from the introduction of Zn_i into the lattice [a donor in ZnO (Refs. 15 and 16)].

To discount the possibility of secondary phase formation in the treated film, both grazing-incidence x-ray diffraction (GIXRD) and x-ray absorption near edge spectroscopy (XANES) were utilized. A portion of a slow GIXRD scan of the Zn-treated film is shown in the inset of Fig. 1(a); a small quantity of polycrystalline ZnO is detected, which may occur in this otherwise epitaxial film due to the large lattice mismatch with the *r*-Al_2O_3 substrate.[17] However, no hint of secondary phase formation is observed. Likewise, the Co *K*-shell XANES spectra presented in Fig. 1(b) indicate Co(II) substitution for Zn(II) in ZnO, with no significant changes in

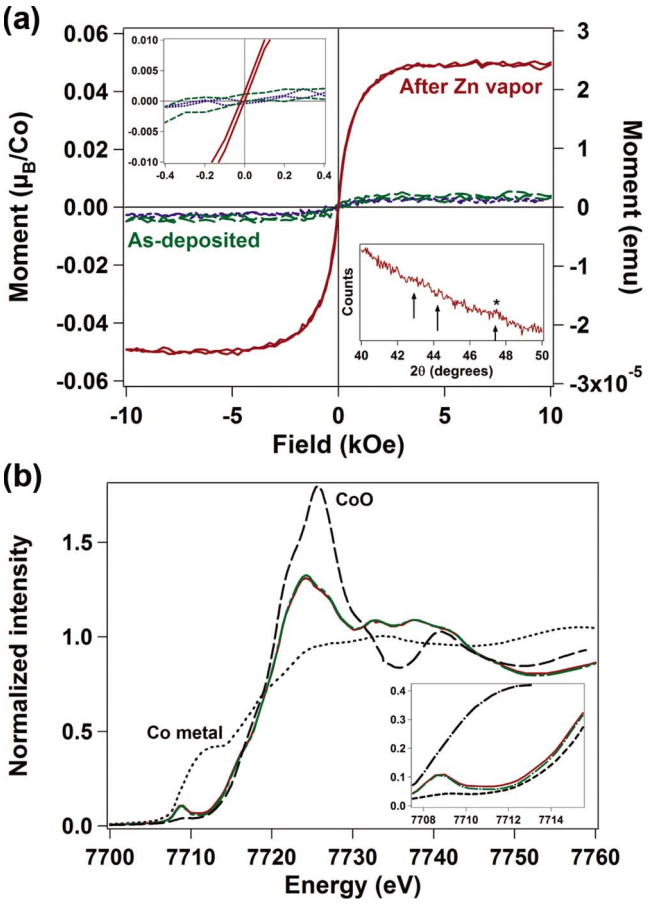

FIG. 1. (Color online) (a) Room temperature VSM of r-Al_2O_3 substrate before deposition (blue dotted line), as-deposited a-Zn_i:$Co_{0.1}Zn_{0.9}O$ film (green dashed line), and film after treatment in Zn vapor (red solid line). Inset: GIXRD pattern of Zn-treated film. The asterisk (*) indicates peak indexed to polycrystalline ZnO. Peak positions of hcp Co(101) at 47.4°, fcc Co(111) at 44.2°, and CoZn(221) at 43.0° are indicated by arrows. (b) Co K-edge XANES of film before (green dash-dot line) and after Zn treatment (red solid line). Reference spectra of Co metal foil (black dashed line) and CoO powder (black dotted line) are included.

the spectral line shape after the Zn treatment. The slight increase in intensity for the Zn-treated film in the "valley" between the preedge 1s-3d feature and the absorption edge, compared to the untreated film, may indicate a very small fraction of Co(0) is present after the Zn treatment. However, the variation in intensity is within the experimental uncertainty of the XANES measurement, and thus cannot be definitively attributed to Co(0) formation.

From the results presented in Fig. 1, it appears conclusive that ferromagnetism is intrinsic to Zn_i:Co:ZnO. However, when incorporating Co as a dopant, there is *always* the possibility of ferromagnetic secondary phase formation which can result in a weak spurious ferromagnetic signal. The very weak ferromagnetism observed after the Zn treatment ($0.05\mu_B$/Co) could result if only 3% of the Co dopants formed Co metal precipitates with a moment of $1.72\mu_B$/Co. Secondary phase formation at this level is far below the detection limit of XRD. Likewise, the detection limit for Co(0) by XANES is estimated to be approximately 5% of the total

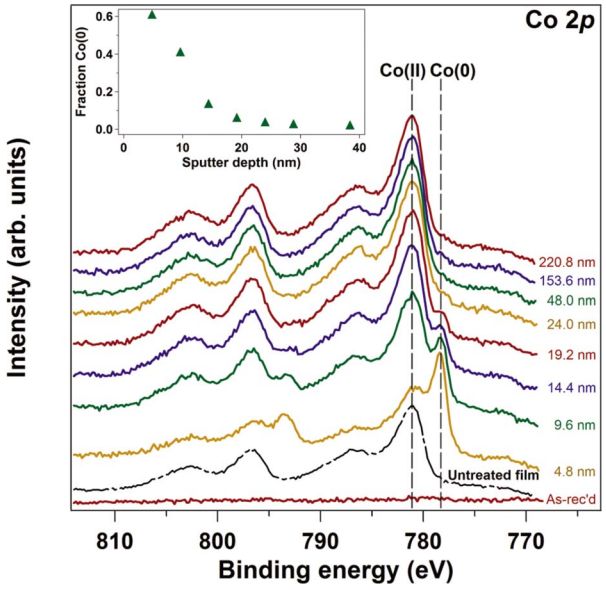

FIG. 2. (Color online) XPS depth profiles of 3100 Å a-$Co_{0.1}Zn_{0.9}O$ after Zn treatment. The vertical dashed lines indicate position of Co(II) at BE=781.1 eV and Co(0) at BE=778.3 eV. For comparison, the Co 2p spectrum of an untreated film after one sputter cycle is shown (dash-dot line) (Ref. 18). Inset: Fraction of Co present as Co(0) as a function of depth in Zn_i:Co:ZnO, as determined by fitting the XPS Co 2p spectra (Ref. 18).

Co.[10] High resolution transmission electron microscopy (TEM) can resolve secondary phase precipitates only a few angstroms in diameter; however, the very small volume sampled by TEM may not be sufficient to detect highly disperse precipitates. Thus, secondary phase formation involving $<5\%$ of the Co dopants would remain undetected by these sophisticated material characterization techniques.

Surface-sensitive spectroscopic techniques can be appropriate to distinguish spatially segregated minority phases. For example, if Co(0) is present and localized near the surface of the Zn_i:Co:ZnO film, it can be readily detected by depth-resolved x-ray photoelectron spectroscopy (XPS). The Co 2p core-level spectrum shows an ~3 eV binding energy shift between Co(0) and Co(II), making charge state identification straightforward. However, due to its surface sensitivity, XPS is generally *not* appropriate to identify Co(0) in Co-doped oxides, since Co near the film surface is likely to be oxidized to Co(II) upon air exposure, regardless of the Co charge state distribution within the film. Argon ion sputter depth profiling can be employed to investigate deeper into the film, provided the physical sputtering does not alter the charge state of Co.[18]

Figure 2 shows selected XPS spectra from the Zn-treated film shown above in Fig. 1. For the as-received film (after Zn vapor treatment), the adventitious carbon contamination is sufficient to completely suppress any signal from Co. After one sputter cycle, which removes 4.8 nm of material, the surface contamination is completely removed, revealing the subsurface Co 2p region. The Co $2p_{3/2}$ consists of two peaks, assigned to Co(II) and Co(0). Peak fitting[18] indicates that approximately 60% of the Co at this depth is Co(0). Further sputtering cycles show a sharp decrease in the fraction of

Co(0). The slight intensity at the Co(0) binding energy in the bulk of the film may be due to the sputtering knock-on of Co(0) from the surface. Thus, it appears that the Zn vapor treatment reduced a significant fraction of Co to Co(0) in the top portion of the film, but did not affect the charge state of the dopant in the bulk of the film. From fits of the XPS spectra, it is estimated that 30% of the Co in the top 20 nm of the film was reduced to Co(0). This corresponds to 2% of the total Co, which is roughly consistent with the estimation of Co metal formation based on magnetometry (3% of the Co, assuming $1.72\mu_B$/Co). Thus, the observed ferromagnetism in these Zn_i:Co:ZnO films originates not from intrinsic magnetic ordering facilitated by Zn_i but from Co(0) generated during Zn vapor treatment. Significantly, the amount of Co(0) present is at a level below the detection limit of most bulk characterization techniques, such as XRD and XANES. It should be noted, however, that due to the differences in Zn vapor treatment, these results do not necessarily imply that the same effect has occurred in previous studies of Zn_i:Co:ZnO.[11–14]

To determine the identity of the Co(0) secondary phase, a 1000 Å Zn_i:Co:ZnO film deposited on r-Al_2O_3 was investigated. Although this film underwent an identical Zn vapor treatment as those presented above (600 °C for 5 h), much more Co(0) was generated. By fitting the XANES data (not shown), ~25% of the total Co was found to be Co(0). This large signal from Co(0) allows a detailed investigation into the nature of the secondary phase via extended x-ray absorption fine structure (EXAFS).

Figure 3(a) shows the Fourier-transformed EXAFS data taken with the linearly polarized x-ray beam oriented both perpendicular and parallel to the film surface. For perpendicular polarization, a strong contribution from Co-M bonding (where M is Co or Zn) is seen, in addition to substitutional Co in ZnO. However, the analogous data in parallel polarization show an apparently reduced contribution from Co-M bonding. Detailed analysis[19] indicates that the secondary phase is the intermetallic $Co_{0.5}Zn_{0.5}$. As illustrated in Fig. 3(b), CoZn takes the β-Mn structure (space group $P4_132$), with a complex 20-atom cubic unit cell in which Co preferentially occupies the 8 M sites of icosahedral coordination, while Zn and the remaining 1/6 Co occupy the 12 T sites which form corner-sharing T_6 octahedra.[20–22] The two Fourier-transformed data sets shown in Fig. 3(a) were simultaneously fit using a theoretical model assuming oriented CoZn(111) embedded in Co:ZnO(001).[19] As seen in Fig. 3(a), the resulting fits reproduce the experimental EXAFS data quite well, including the polarization dependence of the secondary phase signal. Fitting reveals that 25% of the Co is incorporated in CoZn, and the remaining 75% remains substitutional in ZnO. The fit parameters show some discrepancy for Zn_i:Co:ZnO versus those for CoZn powder,[23] which may indicate the presence of Co metal in Zn_i:Co:ZnO as well.[19]

CoZn is ferromagnetic, with a reported saturation moment of $0.8-1.2\mu_B$/Co (Refs. 22 and 24) and a Curie temperature of 400–450 K.[22,25] To confirm, the magnetic properties of CoZn powder were measured by VSM. The hysteresis loop measured at room temperature is given in Fig. 3(b); the measured saturation moment of $1.54\mu_B$/Co is somewhat higher than previously reported.

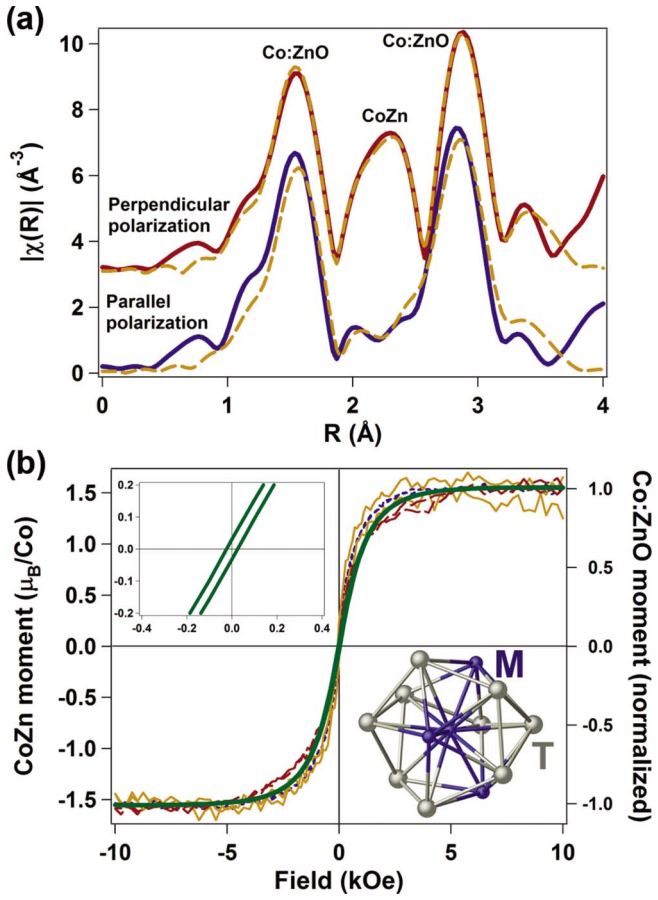

FIG. 3. (Color online) (a) k^2-weighted Fourier-transformed Co K-shell EXAFS of 1000 Å a-Zn_i:$Co_{0.1}Zn_{0.9}O$ with perpendicular (red solid line, top) and parallel (blue solid line, bottom) beam polarizations, along with fits to the data (yellow dashed lines) assuming oriented CoZn(111). (b) Room temperature VSM of polycrystalline CoZn flakes (thick solid green, left axis). Also plotted are normalized VSM hysteresis loops of three Zn_i:Co:ZnO films (right axis). Inset: Structural diagram of CoZn with the β-Mn structure; M (blue or dark gray) and T (light gray) sites are indicated.

While the curvature of the CoZn and the Zn_i:Co:ZnO thin film magnetization loops are similar [Fig. 3(b)], the magnitude of the saturation moments do not correspond to the CoZn content estimated by EXAFS. The film shown in Fig. 3(a) only exhibits 18% of the expected ferromagnetic moment. This suggests that a majority of the CoZn generated in the material has not formed into ferromagnetic clusters, which likely is a diffusion-limited process. The discrepancy is even more striking for the same film deposited on c-sapphire (not shown), which exhibited just 10% of the expected ferromagnetic moment. There appears to be a strong crystalline orientation and/or microstructure dependence on the diffusion and aggregation of reduced dopant atoms in ZnO.

Intermetallic, ferromagnetic CoZn has not been previously explored as a potential secondary phase in Co:ZnO. The thermodynamics of CoZn formation has not been investigated; CoZn may form during deposition or postgrowth processing under low-oxygen or vacuum conditions, even in the absence of Zn vapor. CoZn is a particularly insidious

ferromagnetic secondary phase, since its low moment per Co and low reported Curie temperature [~400–450 K (Refs. 22 and 25)] are in line with the expected properties of ferromagnetic Co:ZnO. Thus, in the absence of careful materials characterization, undetected CoZn could mimic intrinsic ferromagnetism in Co:ZnO.

Although the data presented above focuses on Co:ZnO thin films annealed in Zn vapor, the importance of hidden secondary phase discovery applies to all ferromagnetic Co:ZnO specimens, as well as to other doped oxide systems with potentially ferromagnetic secondary phases. It should be noted, however, that some reported results of ferromagnetism in Co:ZnO, particularly in nanoparticles which were allowed to aggregate at room temperature,[26,27] cannot be easily explained by the presence of undetected secondary phases. Instead, defect-mediated substitutional Co(II) spin coupling has been invoked and defended for these materials.[26,27]

We have shown that, when the ferromagnetic signal is weak, even sophisticated materials characterization techniques may not be sensitive to the small quantity of potential secondary phase involved. Only painstakingly careful materials characterization by several complementary but independent techniques can eliminate the possibility of secondary phase formation in doped oxides such as Co:ZnO.

The authors wish to acknowledge helpful discussions with D. R. Gamelin. This work was performed in the Environmental Molecular Sciences Laboratory, a national scientific user facility sponsored by the Department of Energy's Office of Biological and Environmental Research and located at Pacific Northwest National Laboratory. This work was supported by the U.S. Department of Energy, Office of Science, Office of Basic Energy Sciences, Division of Materials Sciences. Use of the Advanced Photon Source was supported by the U.S. Department of Energy, Office of Science, Office of Basic Energy Sciences under Contract No. DE-AC02-06CH1135.

*tiffany.kaspar@pnl.gov

[1] S. A. Wolf, D. D. Awschalom, R. A. Buhrman, J. Daughton, S. von Molnar, M. L. Roukes, A. Y. Chtchelkanova, and D. M. Treger, Science **294**, 1488 (2001).
[2] T. Dietl, H. Ohno, F. Matsukura, J. Cibert, and D. Ferrand, Science **287**, 1019 (2000).
[3] Y. Matsumoto, M. Murakami, T. Shono, T. Hasegawa, T. Fukumura, M. Kawasaki, P. Ahmet, T. Chikyow, S. Koshihara, and H. Koinuma, Science **291**, 854 (2001).
[4] S. A. Chambers, Surf. Sci. Rep. **61**, 345 (2006).
[5] S. J. Pearton, W. H. Heo, M. Ivill, D. P. Norton, and T. Steiner, Semicond. Sci. Technol. **19**, R59 (2004).
[6] T. Fukumura, H. Toyosaki, and Y. Yamada, Semicond. Sci. Technol. **20**, S103 (2005).
[7] S. J. Pearton, D. P. Norton, M. P. Ivill, A. F. Hebard, J. M. Zavada, W. M. Chen, and I. A. Buyanova, J. Electron. Mater. **36**, 462 (2007).
[8] T. Dietl, J. Phys.: Condens. Matter **19**, 165204 (2007).
[9] R. Janisch, P. Gopal, and N. A. Spaldin, J. Phys.: Condens. Matter **17**, R657 (2005).
[10] T. C. Kaspar, T. Droubay, Y. Li, S. M. Heald, P. Nachimuthu, C. M. Wang, V. Shutthanandan, C. A. Johnson, D. R. Gamelin, and S. A. Chambers, New J. Phys. (in press).
[11] K. R. Kittilstved, D. A. Schwartz, A. C. Tuan, S. M. Heald, S. A. Chambers, and D. R. Gamelin, Phys. Rev. Lett. **97**, 037203 (2006).
[12] D. A. Schwartz and D. R. Gamelin, Adv. Mater. (Weinheim, Ger.) **16**, 2115 (2004).
[13] J. L. MacManus-Driscoll, N. Khare, Y. Liu, and M. E. Vickers, Adv. Mater. (Weinheim, Ger.) **18**, 1449 (2006).
[14] J. L. MacManus-Driscoll, N. Khare, Y. Liu, and M. E. Vickers, Adv. Mater. (Weinheim, Ger.) **19**, 2925 (2007).
[15] L. E. Halliburton, N. C. Giles, N. Y. Garces, M. Luo, C. Xu, L. Bai, and L. A. Boatner, Appl. Phys. Lett. **87**, 172108 (2005).
[16] D. G. Thomas, J. Phys. Chem. Solids **3**, 229 (1957).
[17] C. R. Gorla, N. W. Emanetoglu, S. Liang, W. E. Mayo, Y. Lu, M. Wraback, and H. Shen, J. Appl. Phys. **85**, 2595 (1999).
[18] See EPAPS Document No. E-PRBMDO-77-R04820 for additional experimental details and XPS data. For more information on EPAPS, see http://www.aip.org/pubservs/epaps.html.
[19] S. M. Heald (unpublished).
[20] T. J. Prior, D. Nguyen-Manh, V. J. Couper, and P. D. Battle, J. Phys.: Condens. Matter **16**, 2273 (2004).
[21] C. B. Shoemaker, D. P. Shoemaker, T. E. Hopkins, and S. Yindepit, Acta Crystallogr., Sect. B: Struct. Crystallogr. Cryst. Chem. **B34**, 3573 (1978).
[22] T. Hori, H. Shiraish, and Y. Ishii, J. Magn. Magn. Mater. **310**, 1820 (2007).
[23] Powders synthesized at the Materials Preparation Center, Ames Laboratory, USDOE, see www.mpc.ameslab.gov
[24] K. H. J. Buschow, P. G. van Engen, and R. Jongerbreur, J. Magn. Magn. Mater. **38**, 1 (1983).
[25] I. Isomäki and M. Hämäläinen, J. Alloys Compd. **375**, 191 (2004).
[26] P. V. Radovanovic and D. R. Gamelin, Phys. Rev. Lett. **91**, 157202 (2003).
[27] D. A. Schwartz, N. S. Norberg, Q. P. Nguyen, J. M. Parker, and D. R. Gamelin, J. Am. Chem. Soc. **125**, 13205 (2003).